CONF-791102-15

LA-UR-79-2862

TITLE: APPLICATION OF NUCLEAR MODELS

AUTHOR(S): P. G. Young, E. D. Arthur, and D. G. Madland

SUBMITTED TO:

International Conference on Nuclear Cross Sections for Technology
Knoxville, TN
October 22-26, 1979

MASTER

los alamos scientific laboratory
of the University of California
LOS ALAMOS, NEW MEXICO 87545

APPLICATION OF NUCLEAR MODELS

P. G. Young, E. D. Arthur, and D. G. Madland
Los Alamos Scientific Laboratory, University of California
Theoretical Division
Los Alamos, New Mexico 87545 U.S.A.

The development of our extensive experimental nuclear data base over the past three decades has been accompanied by parallel advancement of nuclear theory and models used to describe and interpret the measurements. This theoretical capability is important because of many nuclear data requirements that are still difficult, impractical, or even impossible to meet with present experimental techniques. Examples of such data needs are neutron cross sections for unstable fission products, which are required for neutron absorption corrections in reactor calculations: cross sections for transactinide nuclei that control production of long-lived nuclear wastes and the extensive dosimetry, activation, and neutronic data requirements to 40 MeV that must accompany development of the Fusion Materials Irradiation Test (FMIT) facility. In recent years systematic improvements have been made in the nuclear models and codes used in data evaluation and, most importantly, in the methods used to derive physically based parameters for model calculations. The newly issued ENDF/B-V evaluated data library relies in many cases on nuclear reaction theory based on compound-nucleus Hauser-Feshbach, preequilibrium and direct reaction mechanisms as well as spherical and deformed optical-model theories. The development and applications of nuclear models for data evaluation are discussed in this paper, with emphasis on the 1-40 MeV neutron energy range.

Introduction

The requirements for evaluated nuclear data that result from the various nuclear applications are sufficiently broad that the use of nuclear theory and models is essential to complement the available experimental data base. A number of areas exist where nuclear models play a very important role. A classic example is the problem of determining nuclear data for radioactive or unstable target nuclei which, of course, are very difficult to measure and which are required in a number of applications. Such applications include calculation of neutron absorption and scattering by fission products in thermal and fast reactors; production, depletion, and absorption calculations for actinide nuclides important in waste management and disposal studies; and activation calculations for fusion reactor components and shielding that can involve unstable intermediate nuclei. A second area where nuclear models are very important is the extension of the evaluated data base into the 20-50 MeV incident neutron energy range, where experimental data are much more limited than at lower energies. Although biomedical and shielding data needs have existed in this region for many years, the planned development of d + Li neutron sources, such as the Fusion Materials Irradiation Test facility (FMIT), has given new impetus to developing evaluated data libraries above 20 MeV. It should also be mentioned that in the more common applications models still play an important role in interpolating and extrapolating data such as secondary angular and energy distributions that have not been measured with the same thoroughness as energy-dependent cross sections. For example, the energy range between 9-14 MeV is only sparsely measured for many nuclei. Finally, nuclear models have advanced to a state that they can occasionally be useful to evaluators in deciding among discrepant experimental results.

The use of nuclear theory in data evalations has expanded and become more sophisticated over the years in much the same way that the experimental data base has developed. In this paper we will outline some of the advances that have occurred in the recent past in applying nuclear theory and models to data evaluation. We will describe briefly some of the features of nuclear model codes in common use and will show examples of their application in recent evaluations. Because of time and space limitations, we will restrict the discussion mainly to neutron-induced and fusion reactions in the 1-40 MeV energy region, which excludes the resolved and unresolved resonance regions for the heavier nuclei. We will close with some observations and comments on the recently issued Version V of ENDF/B.

Use of Nuclear Theory in Light Element Evaluations

Nuclear models used in evaluation range from the almost trivially simple to the very complex, depending upon what is appropriate and available for a given situation. An example of the former is the use of simple three-body phase space calculations to represent secondary energy distributions from breakup of light systems. This technique is used in the ^{6}Li ENDF/B-V evaluation[1] to represent the continuum part of the neutron spectrum from the ^{6}Li(n,nd)^{4}He reaction, as illustrated in Fig. 1. Note that elastic scattering is omitted from the calculated curves in Fig. 1. The calculated spectral shape agrees reasonably with the experimental data and provides a useful device for inferring the spectra at unmeasured energies and angles. There are many light nuclei, however, for which such simple representations are unsatisfactory.

At the other end of the complexity scale is the use of sophisticated coupled-channel R-matrix analyses in data evaluations. Such analyses are incorporated in the ENDF/B-V evaluations for ^{4}He, ^{6}Li, ^{10}B, ^{12}C, and ^{16}O, which include the three standard reactions ^{6}Li(n,t)^{4}He, ^{10}B(n,α)^{7}Li and ^{12}C(n,n)^{12}C.

While such applications of R-matrix theory are not new, it is only in relatively recent times that analyses of sufficient detail and thoroughness have been available for light systems so that accurate predictions of results can be made in poorly measured reaction channels of a system. Additionally, by application of the principle of charge independence, predictions can now be extended to different isospin members of a mass system.[2] Such analyses are proving most helpful in providing charged-particle fusion data, and a list of reactions analyzed in this manner at Los Alamos Scientific Laboratory (LASL) library is included in Table I. Be-

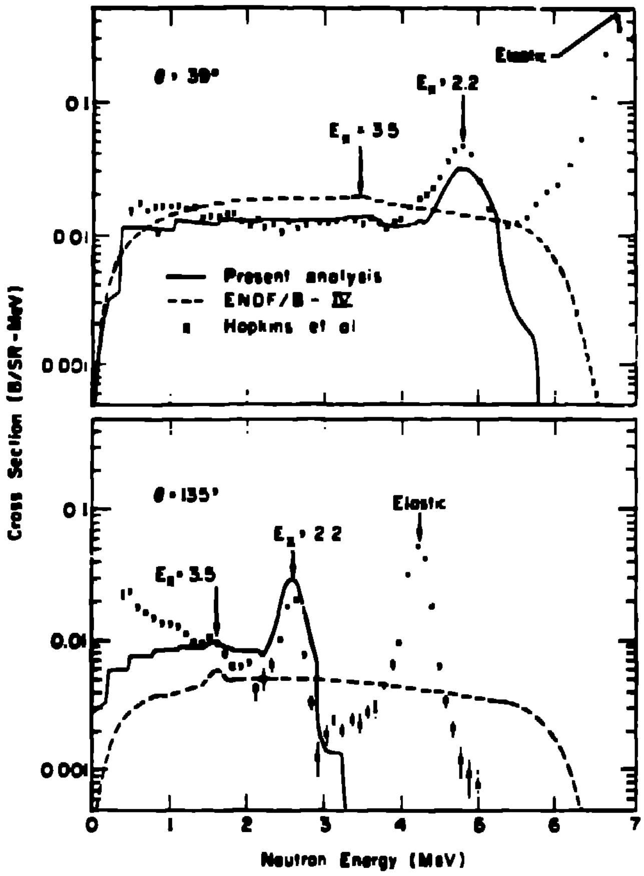

Fig. 1. Neutron emission spectra at laboratory angles of 39 and 135° from 5.74-MeV neutron bombardment of ^{6}Li. As described in Ref. 1, the calculated curves do not include elastic scattering.

Because this topic is the subject of another talk[3] at this conference, no further discussion is included here.

Nuclear Models for Intermediate and Heavy Mass Evaluation

The nuclear models and theories most commonly applied in evaluations of neutron-induced data for heavier nuclei in the MeV region are the spherical and deformed optical models, Hauser-Feshbach statistical theory, direct reaction theory, preequilibrium theory, and fission theory. A number of theoretical improvements have occurred over the past few years, and some of these are cited below. Equally important for data evaluation, however, has been the development and use of improved methods for determining parameters used in model calculations and the coming of age of several multistep Hauser-Feshbach/preequilibrium theory codes that can accomodate the myriad of reaction channels open at incident neutron energies of 20 MeV and higher.

Optical Model Parameterizations

The optical model is still one of the most important tools for a good theoretical evaluation, whether dealing with spherical or deformed target nucleus. In addition to providing a means to calculate energy dependent total, elastic, and reaction cross sections as well as elastic angular distributions, it is also used to compute transmission coefficients that are used in Hauser-Feshbach or direct reaction calculations. There has been increasing recognition over the past several years that the old global or universal parameter sets such as the Wilmore-Hodgson,[4] Perey,[5] or Becchetti-Greenlees[6] parameters, while very useful for scoping calculations of specific nuclei. It is far preferable to use optical model parameters that are optimized over a more limited region of A, such as a particular shell, at the same time preserving the accepted trends with energy and mass of the parameters. As a result, there has been a renewal of efforts to determine realistic optical parameters for evaluations over the past few years.

A very useful technique for obtaining neutron optical parameters for spherical and deformed nuclei that does not require exteneivie automated least-squares fitting and can therefore be performed with modest computing outlay has been developed at Bruyeres-le-Chatel by Lagrange and his coworkers.[8] This technique, referred to as the "SPRT" method, uses s- and p-wave strength functions and the potential scattering radius as data to aid in determination of the real and (surface) imaginary potentials at low energies and then uses the total cross section to establish their energy dependence. Fine tuning of the potential is accomplished by adjusting the spin-orbit strength to match back angle elastic scattering data and the imaginary strengths to match inelastic scattering cross sections. Proton elastic scattering and polarization data can then be analyzed using the derived neutron parameters to provide further information concerning isospin terms, higher energy behavior, etc. The end results are nucleon optical parameters suitable for use over an expanded energy range for a nucleus or nuclei of interest. Such an analysis for ^{93}Nb is reported at this conference[9] with an example of the quality of fit to proton polarization data shown in Fig. 2.

A second technique that also averts extensive fitting for deformed nuclei has been developed by

Table I. Charged-Particle Reactions For Which Cross Sections Are Available From Current LASL R-Matrix Analyses

Reaction	Energy Range (MeV)
T(p,p)T	E_p = 0-11
T(p,n)^{3}He	E_p = 1-11
^{3}He(p,p)^{3}He	E_p = 0-20
^{4}He(p,p)^{4}He	E_p = 0-3[illegible]
^{6}Li(p,p)^{6}Li	E_p = 0-2.5
^{6}Li(p,α)^{3}He	E_p = 0-2.5
D(d,d)D	E_d = 0-10
D(d,n)^{3}He[a]	E_d = 0-10
D(d,p)T[a]	E_d = 0-10
T(d,d)T	E_d = 0-8
^{3}He(d,d)^{3}He	E_d = 0-10
^{3}He(d,p)^{4}He	E_d = 0-10
^{4}He(d,d)^{4}He	E_d = 0-15
T(t,t)T	E_t = 0-2
T(t,2n)^{4}He	E_t = 0-2
^{4}He(t,t)^{4}He	E_t = 0-14
^{4}He(t,n)^{6}Li	E_t = 0-14
^{4}He(^{3}He,^{3}He)^{4}He	$E_{^3He}$ = 0-11

[a]Results preliminary.

Madland.[7] With this method, parameters are determined for a spherical optical potential, which is relatively inexpensive to compute, by fitting all available total and differential elastic scattering data. Simple transformations are then sought that will result in realistic deformed model parameters by fitting a much more restricted data set in a fully deformed coupled-channel optical model calculation.

Preliminary results from such an analysis were reported at Harwell[7] and are reproduced in Fig. 3. The solid curves represent neutron total cross sections calculated with a spherical optical model determined by fitting experimental data for all five actinides in Fig. 3. The dashed curve shown for ^{238}U was obtained in a deformed calculation using a simple parameter transformation determined by simultanteously fitting ^{238}U inelastic angular distributions at only two energies (1.5 and 3.4 MeV). The ^{238}U total cross sections calculated with the deformed model agree with experiment to within ± 3% for neutron energies between 50 keV and 10 MeV. Additionally, the geometrical parameters obtained in this analysis are reasonably similar to ones obtained by Lagrange[10,11] using the SPRT method.

Gamma-Ray Strength Functions

Another important aspect of model calculations is to properly describe gamma-ray emission, both in estimating gamma competition to particle emission and fission in Hauser-Feshbach calculations and in actually computing gamma-ray emission spectra for use in evaluations. In most Hauser-Feshbach calculations, the integral of the product of level density and gamma-ray transmission coefficients is normalized to the experimental value of $2\pi\langle\Gamma_\gamma\rangle/\langle D\rangle$, where $\langle\Gamma_\gamma\rangle$ and $\langle D\rangle$ are the average gamma width and spacing for s-wave resonances. This normalization directly influences the amount of gamma-ray emission occurring, either in the capture reactions or in competition to particle-emission or fission reactions. Experimental data for $\langle\Gamma_\gamma\rangle$ and $\langle D\rangle$ are not always reliable (especially where resonance spacings are large), and for compound systems lacking such data, reliance must be placed upon determination of these quantities from systematics. Since the observed spacing $\langle D\rangle$ can vary can vary drastically between nearby nuclei in closed shell regions, considerable uncertainty can exist in calculations of gamma-ray emission.

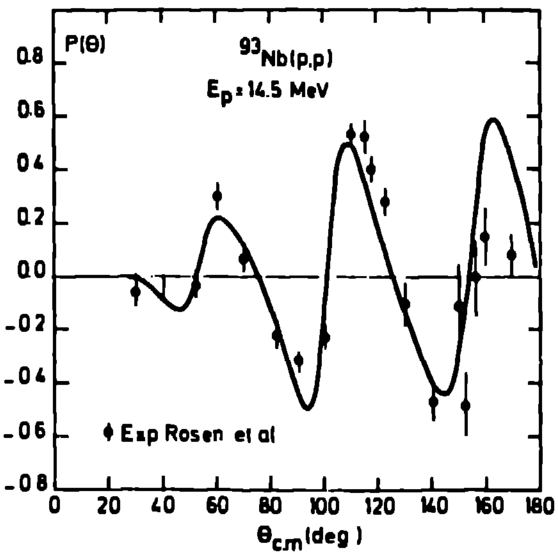

Fig. 2. Calculated and measured proton polarization from ^{93}Nb(p,p) elastic scattering at 14.5 MeV. See Ref. 9 for details.

An alternate approach has been suggested by Gardner[12] that eliminates many of these problems, leading in turn to more accurate capture cross sections where data is unavailable and to a better treatment of gamma-ray competition. This method is based upon determination of the gamma-ray strength function $f(\varepsilon_\gamma)$ defined by

$$\frac{\langle\Gamma_\gamma\rangle}{\langle D\rangle} = \int_0^{S_n} f(\varepsilon_\gamma)\,\varepsilon_\gamma^3\,\rho(S_n-\varepsilon_\gamma)\,d\varepsilon_\gamma \quad , \qquad (1)$$

where S_n is the neutron separation energy, ε_γ is the gamma-ray energy, and ρ is the level density of the compound system. The electric dipole strength function is assumed to have a giant dipole resonance (GDR) form given by

$$f_{E1}(\varepsilon_\gamma) = \frac{k\varepsilon_\gamma\Gamma_{GDR}}{(\varepsilon_\gamma\Gamma_{GDR})^2 + (\varepsilon_\gamma^2-E_{GDR}^2)^2} \quad . \qquad (2)$$

The strength function can be extracted from the analysis of neutron capture cross sections measured for stable nuclei or through the analysis of spectral data resulting from capture. Since the strength function is expected to vary smoothly between nearby nuclei, some of the problems mentioned earlier can be eliminated, and one can use it with increased confidence.

An application of this technique by Gardner[12] for the ^{85}Rb(n,γ) and ^{87}Rb(n,γ) reactions is shown in Fig. 4. The same strength function $f_{E1}(\varepsilon_\gamma)$ was used for both reactions shown in Fig. 4; the vastly different capture cross sections result entirely from the different binding energies and level densities used in the two cases.

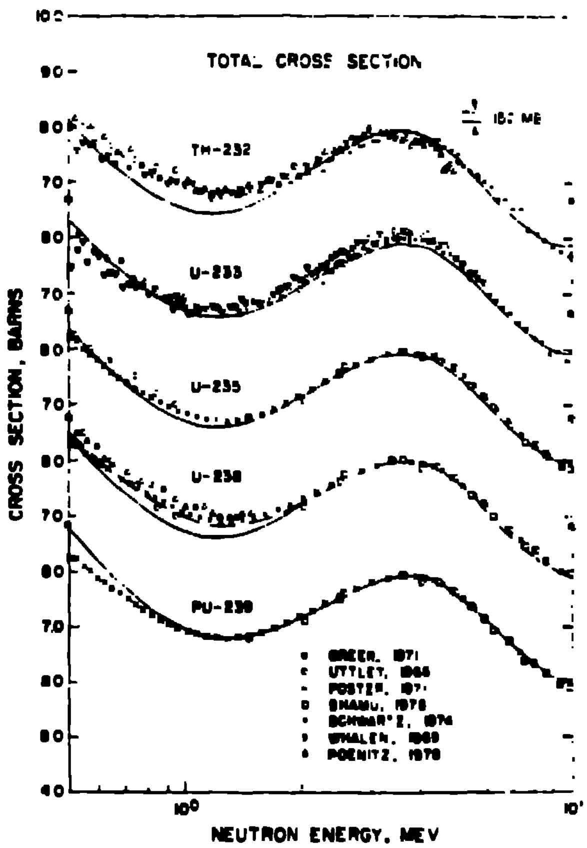

Fig. 3. Calculated and measured neutron total cross sections for five actinide nuclei. See Ref. 7.

Improved Codes for Evaluations

A large number of codes useful for evaluations has been developed in many countries, but space does not permit a thorough discussion here.

One major advance in the past several years that will be discussed, however, is the development of several multistep Hauser-Feshbach statistical-preequilibrium codes that permit calculation of most important reactions in the MeV region. Within the community of ENDF/B evaluators, these codes include the HAUSER[13] code developed at Hanford Engineering Development Laboratory, the TNG[14] code from Oak Ridge National Laboratory, the STAPRE[15] code written in Austria and extensively used at Lawrence Livermore Laboratory and Brookhaven National Laboratory, and the GNASH[16] code developed at LASL. These codes, when used in combination with spherical and deformed optical model codes and the older reaction theory code COMNUC,[17] provide a capability for calculating all important reaction sequences up to 20 MeV or higher.

Typical reaction sequences that can be included in multistep calculations are shown in Fig. 5. The case illustrated is for neutron-induced reactions on ^{89}Y, which were recently calculated with the GNASH code.[18] The double arrows indicate the path from the incident channel to the first compound nucleus $^{90}Y^*$, whose decays correspond to the binary (n,γ), (n,p), (n,α), and (n,n') reactions. The various compound nuclei shown in the diagram are populated in specific energy, spin, and parity states, and each nucleus is permitted to decay by n, p, α, and/or γ emission until the decay sequences terminate. The most complicated sequences shown in Fig. 5 are (n,2nγ), (n,2np), (n,2nα), and (n,3n) reactions, although calculations are not limited to these.

All four multistep Hauser-Feshbach codes mentioned above can carry out these calculations with full allowance for angular momentum effects. The TNG, HAUSER, and STAPRE codes include width fluctuation corrections for the lower energy calculations, whereas GNASH, which is designed for higher energy calculations does not. All four codes include preequilibrium models that are used to correct the binary reactions for nonequilibrium effects. In the case of TNG, a new model (described in a later paper[19]) has been included to incorporate conservation of angular momentum in the preequilibrium step. This model ensures consistency between the statistical and preequilibrium parts of the calculations. Particle spectra are calculated in all four codes, and all except HAUSER also output gamma-ray spectra. The HAUSER, GNASH, and TNG codes allow input of externally computed direct-reaction cross sections to specific states, which are combined with the Hauser-Feshbach calculations and, in the case of GNASH and TNG, are included explicitly in the gamma-ray cascades. The TNG and HAUSER codes calculate compound nucleus angular distributions, whereas GNASH and STAPRE rely upon external codes for these effects. STAPRE, HAUSER, and GNASH all have fission channels, with a double-humped barrier being available for use in HAUSER and STAPRE.

In the past few years these codes have been extensively developed and used in support of data evaluation, and examples of calculations are given below. The Nuclear Models Subcommittee of the Cross Section Evaluation Working Group has been carrying out code comparison studies with these and other codes, and even more detailed comparisons have been made between codes used at LLL and LASL.[20]

Examples of Recent Calculations

There are a number of examples that can be cited where the above codes have been successfully applied to evaluation problems. The HAUSER code has been used extensively by Mann and Schenter[21] in calculations of actinide cross sections for ENDF/B-V. Similarly, Fu has used TNG for ENDF/B evaluations of ^{40}Ca,[22] ^{56}Fe,[23] and Pb,[24] and for Cu and Nb calculations to 32 MeV.[25] Calculations with STAPRE include comprehensive analyses by M. Gardner of neutron-induced reactions on zirconium isotopes[26] and by D. Gardner of neutron reactions on 33 target states of $^{175,176}Lu$.[27] Additionally, an analysis[28] of neutron reactions on barium isotopes with STAPRE h

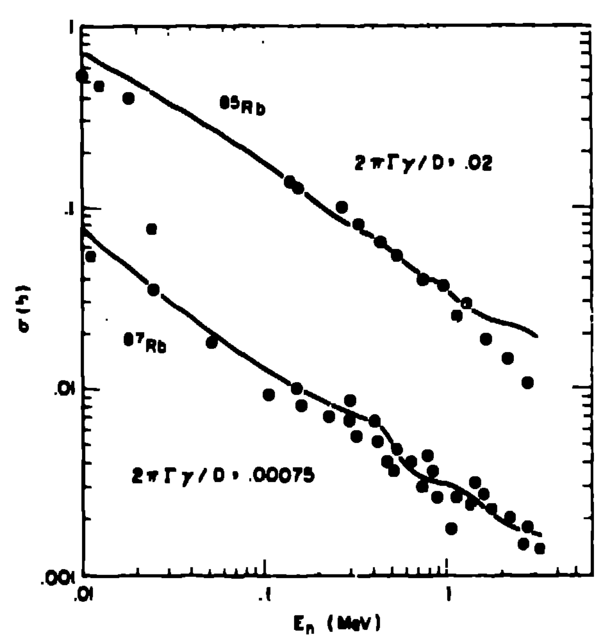

Fig. 4. Rb(n,γ) and Rb(n,γ) cross sections between 10 keV and 3.5 MeV. See Ref. 12 for details.

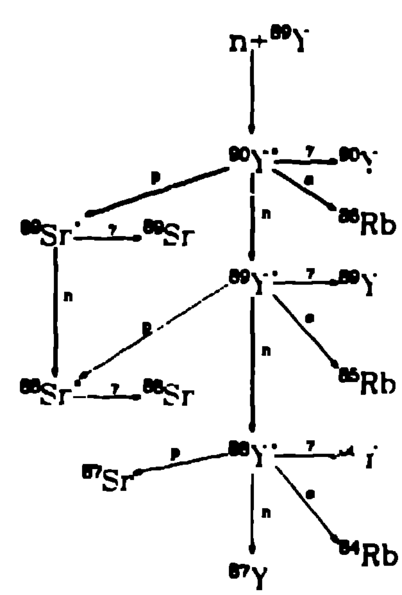

Fig. 5. Sample reaction decay sequences from neutron interactions with ^{89}Y as calculated by Arthur (Ref. 18).

STAPRE have been performed. Recent analyses with the GNASH code include studies of neutron-induced reactions to 20 MeV on a total of 10 isotopes of yttrium and zirconium,[18] to 40 MeV for ^{54}Fe and ^{56}Fe,[29] to 20 MeV for the four principal isotopes of tungsten,[30] and to 22 MeV for ^{235}U and ^{238}U.[31]

To illustrate the potential of such calculations when care is taken with parameterizations, Figs. 6–8 show comparisons between calculated and experimental cross sections from the GNASH analysis of yttrium and zirconium isotopes.[18] In this study, consistency was required of the optical model parameterizations for all the yttrium and zirconium isotopes, and several different types of neutron and charged-particle experiments were fit to determine optical parameters. In addition, a careful study was made using Gardner's method[12] to obtain reliable gamma-ray strength functions.

Gamma-ray energy spectra from GNASH calculations[29] for iron are compared to the experimental data of Chapman et al.[32] at four incident neutron energies in Figs. 9-12. In this case, the model parameters were determined entirely from other measurements, so the comparisons with the gamma-ray spectra provide a test of the calculations. Although the calculations agree relatively poorly with the Chapman data at 14.55 MeV (Fig. 11, they are in reasonably good agreement with the data of Drake et al.[33] at 14.2 MeV, shown in Fig. 13. Thus, there appears to be a discrepancy between the two experiments near 14 MeV, and Arthur's calculations tend to support Drake's measurement.

The neutron emission spectra calculated for 36-MeV neutrons incident on iron are shown at 0, 90, and 180° in Fig. 14. The high energy lines in the spectrum result from Fe(n,n') reactions to discrete states, which were obtained in DWBA calculations and are strongly forward peaked. The angular distributions in the continuum region were calculated from semiempirical relationships determined by Kalbach[?] and based on preequilibrium theory. The breaks in the spectrum in the continuum region indicate the boundaries of 5-MeV wide secondary energy bins, each of which was given a separate angular distribution from the Kalbach formalism. This representation results from an ad hoc modification of the ENDF/B format to accomodate the pronounced forward peaking of spectra at energies above 20 MeV.

The gamma-ray emission spectrum that is calculated for 40-MeV incident neutrons is shown in Fig. 1?. Isotropy was assumed for all emitted gamma rays, and the standard ENDF/B formats were adequate to represent the calculations.

Finally, a comparison of calculated fission[?] cross sections for ^{235}U and ^{238}U with experimental data is shown in Fig. 16. In this case, a simple single-hump fission barrier model in the GNASH code was optimized to the data shown, for the purpose of providing adequate fission competition in calculations of (n,xn) reactions.

Comments on ENDF/B-V

The new multistep Hauser-Feshbach codes and the older direct reaction and compound nucleus theory codes provide a very useful array of tools for optimizing data evaluations. It is usually preferable in cases where measurements are available to base evaluated total and fission cross sections on direct experimental data. In such cases, the use of nuclear models can ensure consistency of the remaining evaluated cross sections through deviation of parameters which simultaneously describe all channels. Evaluations determined with this match of theory and experiment offer the advantage that the neutron, gamma-ray, and charged-particle data satisfy the basic requirements of conservation of total energy and flux.

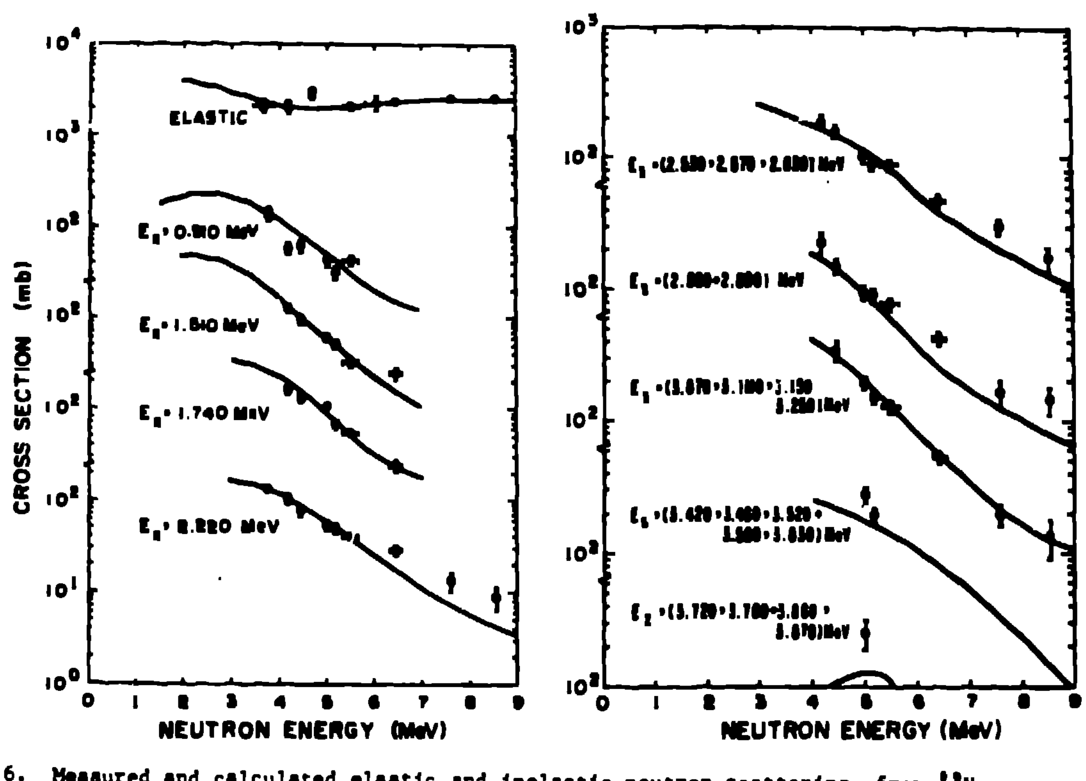

Fig. 6. Measured and calculated elastic and inelastic neutron scattering from ^{89}Y. See Ref. 18 for details.

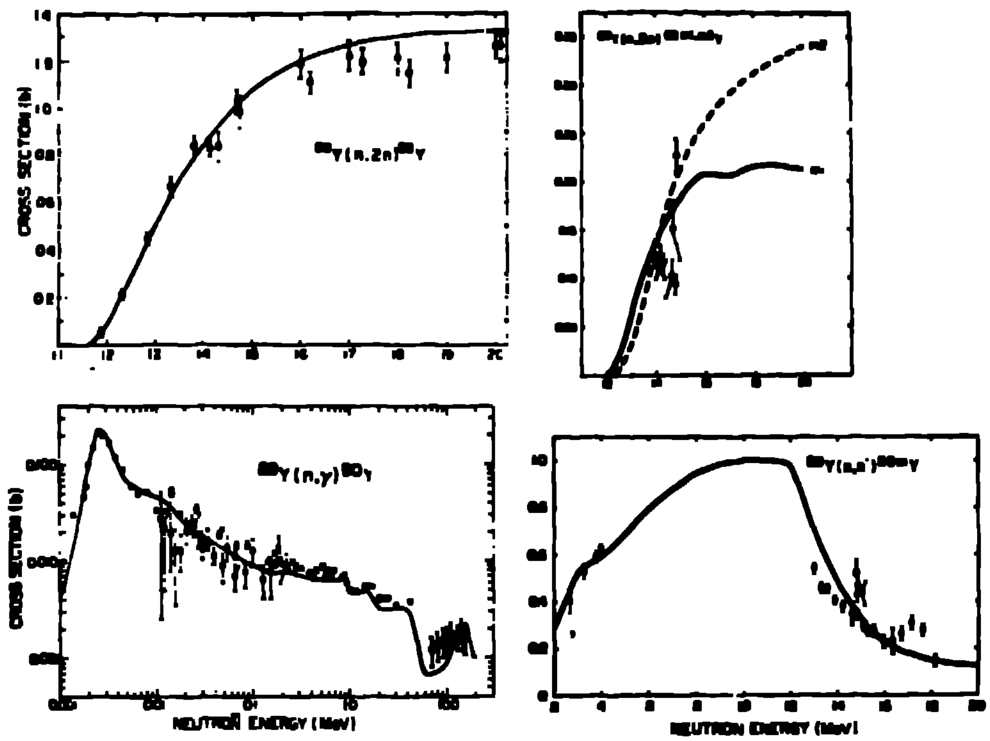

Fig. 7. Measured and calculated cross sections for the ^{88}Y(n,γ)^{89}Y, ^{88}Y(n,n')^{88m}Y, ^{88}Y(n,2n)^{87}Y, and ^{88}Y(n,2n)^{87m1,m2}Y reactions. See Ref. 18 for details.

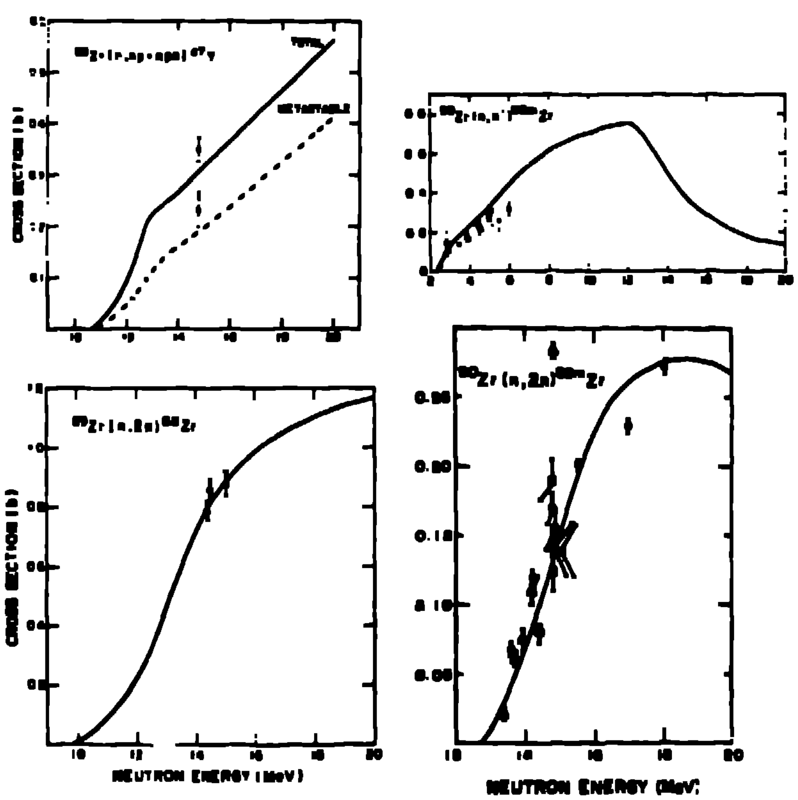

Fig. 8. Measured and calculated cross sections for the ^{88}Zr(n,np)^{87}Y, ^{89}Zr(n,2n)^{88}Zr, ^{89}Zr(n,n')^{89m}Zr, and ^{89}Zr(n,2n)^{88m}Zr reactions. See Ref. 18 for details.

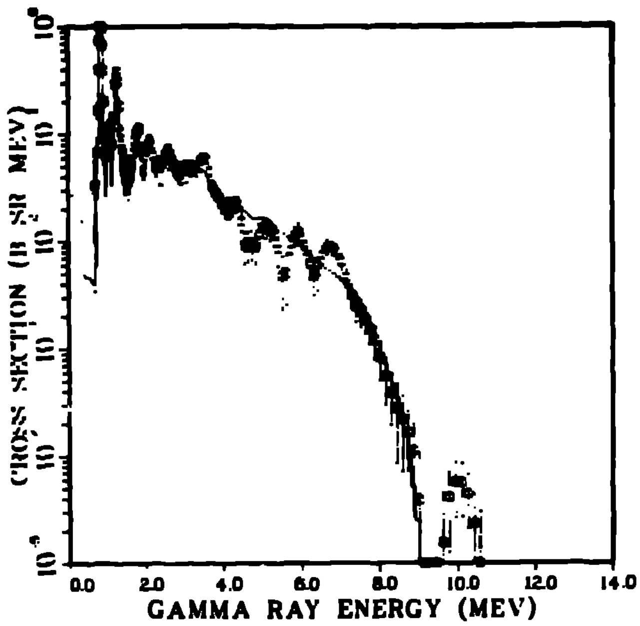

Fig. 9. Calculated gamma-ray emission spectra for 8.76-MeV bombardment of Fe compared to the measurement by Chapman et al. (Ref. 32) at 125°.

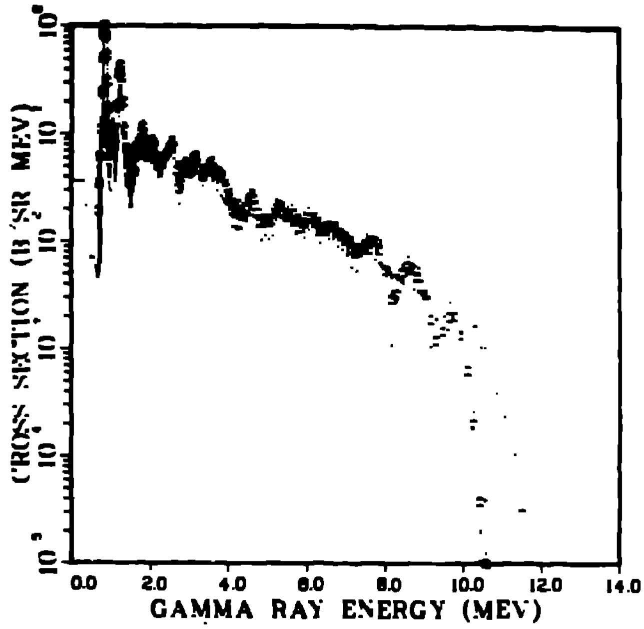

Fig. 10. Calculated gamma-ray emission spectra for 11.5-MeV bombardment of Fe compared to the measurement by Chapman et al. (Ref. 32) at 125°.

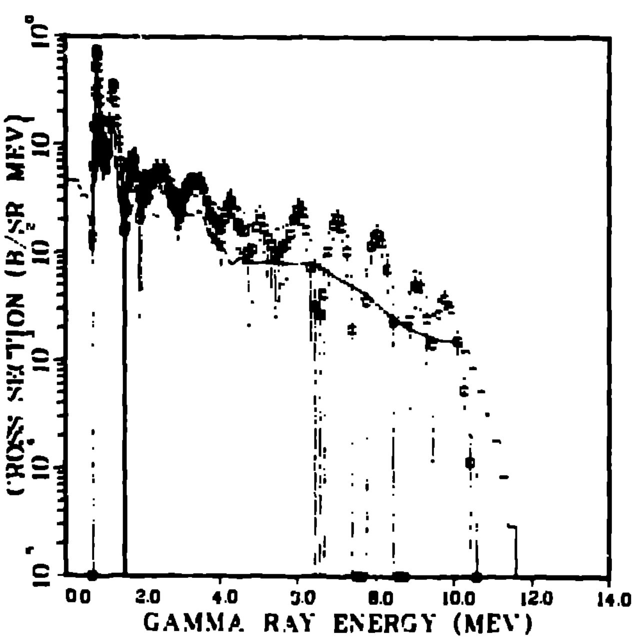

Fig. 11. Calculated gamma-ray emission spectra for 14.55-MeV bombardment of Fe compated to the measure ment by Chapman et al. (Ref. 32) at 125°.

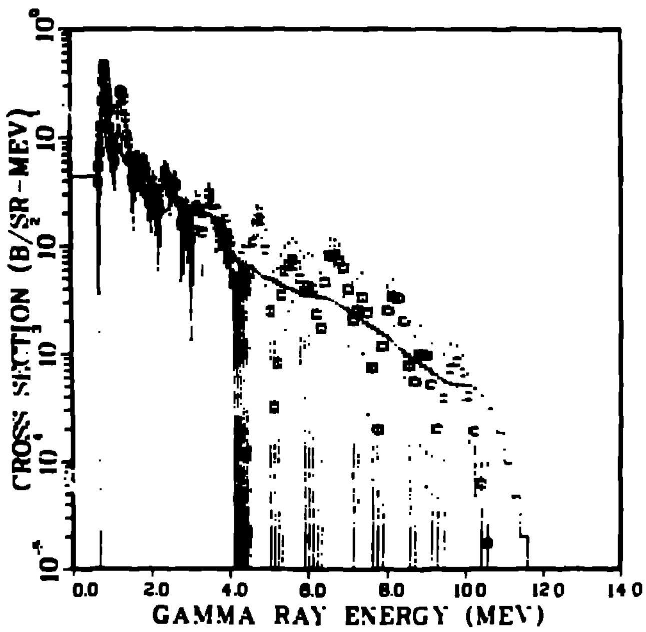

Fig. 11. Calculated gamma-ray emission spectra for 18.85-MeV bombardment of Fe compared to the measure ment by Chapman et al. (Ref. 32) at 125°.

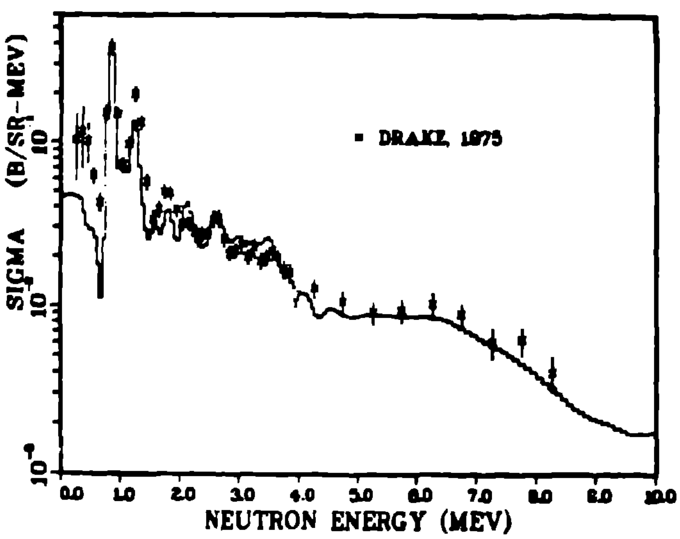

Fig. 13. Calculated gamma-ray emission spectra for 14.2-MeV neutron bombardment of Fe compated to the measurement of Drake et al. (Ref. 33) at 90°.

While nuclear theory has been frequently put to good use in evaluations, its application has tended to be somewhat piecemeal with the result that energy conservation has frequently not been satisfied. Examples of this problem are provided in a recent study of energy balance in ENDF/B-V evaluations by MacFarlane.[35] KERMA factors, which are simply the energy given to charged reactions products, were computed for a variety of non-fissile nuclei at a selection of incident energies by subtracting the energy carried away by neutrons and protons from the total energy (E+Q) available to each reaction. Lower and upper limits based on general considerations were determined for the KERMA factors for most reactions, and tests were made to see if the ENDF/B-V data satisfied the limits.

MacFarlane's results are reproduced in Table II where each evaluation tested us rated as G (good), F (fair), or P (poor) for the energy ranges THER (E_n 1 keV), FAST (1 keV-2MeV), and FUSN (2-20 MeV). A rating of "P" means that KERMA factors computed in this manner are inadequate for most applications and indicates rather significant (1-10%) violations of conservation of total energy.

A disturbing number of "P" ratings occur in Table II. While the KERMA diagnostic is quite sensitive and can indicate rather small violations of energy conservation, a number of cases flagged in Table II do represent significant problems. Additionally, one might take the point of view that conservation of energy should be essentially inviolate in evaluations, in much the same manner that evaluators require that all neutron cross sections sum to the total cross section. Careful, consistent use of nuclear theory in fitting experimental data can help remove problems of this nature in future evaluations.

Summary

Significant advances have occurred over the past several years in applying nuclear theory to data evaluations. Areas highlighted here are the use of R-matrix theory for improving and extending light element evaluations, development of improved methods for determining model parameters, and the availability of several new

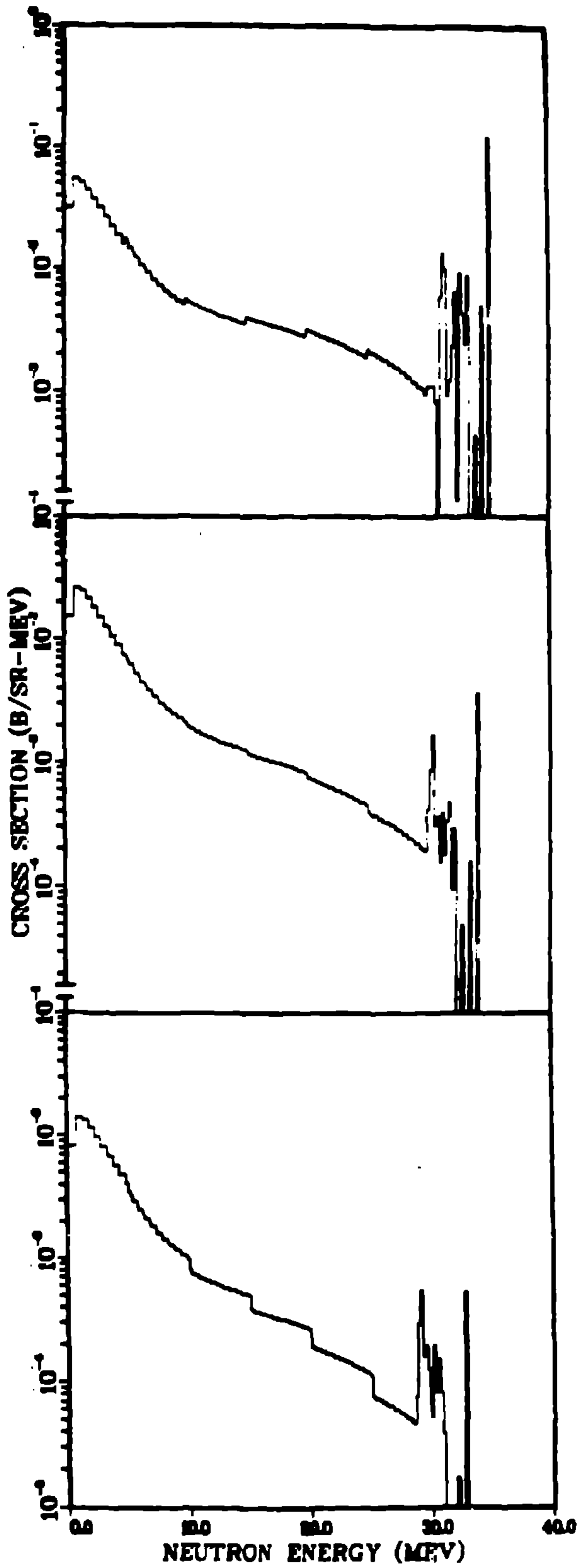

Fig. 14. Calculated neutron emission spectra at 0, 90, and 180° from 36-MeV neutron bombardment of Fe.

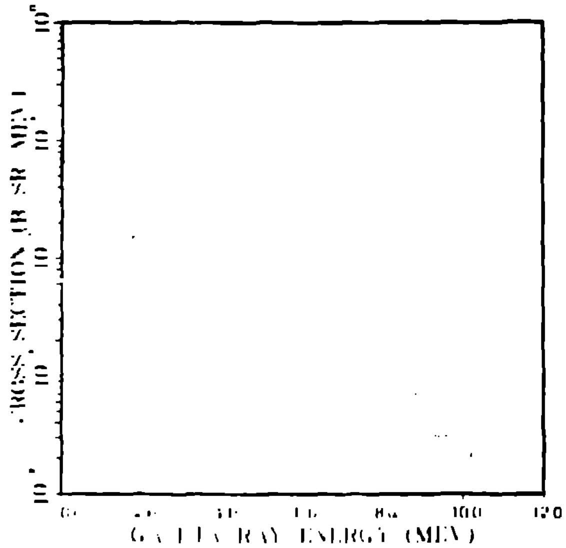

Fig. 15. Calculated gamma-ray emission spectrum from 40-MeV neutron bombardment of Fe.

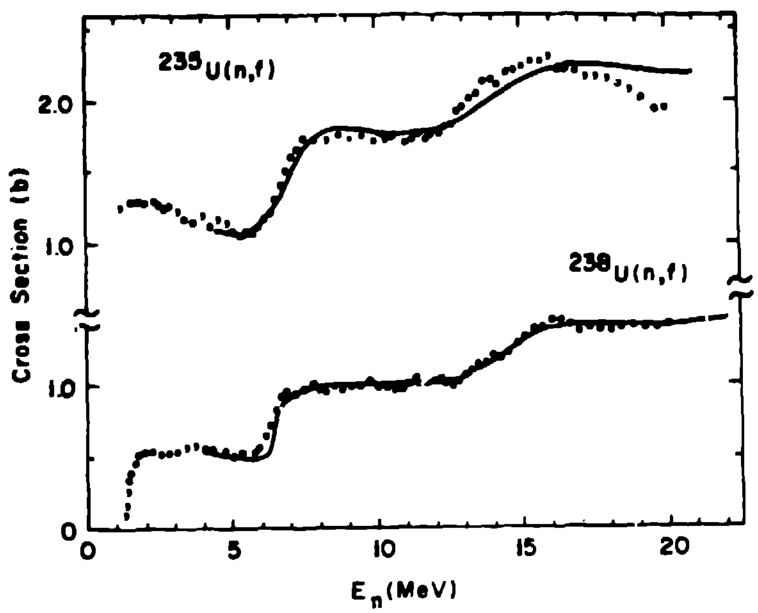

Fig. 16. Measured and calculated ^{235}U(n,f) and ^{238}U(n,f) cross sections. See Ref. 31 for details.

TABLE II

QUALITATIVE RATING OF ENERGY BALANCE FOR MATERIALS FROM ENDF/B-V
(G=Good, F=Fair, P=Poor) BY ENERGY RANGE
(THER<1 keV, FAST=1 keV to 2 MeV, FUSN=2 to 20 MeV)

Material	THER	FAST	FUSN	Material	THER	FAST	FUSN
H-1	G	G	G	K	*	*	P
H-2	G	G	G	Ca	G	G	G
Li-6	G	G	G	Ti	G	F	F
Li-7	G	G	G	V	G	G	F
Be-9	G	G	G	Cr	*	*	P
B-10	G	G	G	Mn-55	P	P	P
C	G	G	G	Fe	*	F	P
N-14	G	G	G	Co-59	G	P	P
N-15	G	G	F	Ni	G	P	F
O-16	G	G	G	Cu	*	*	*
F-19	G	G	F	Mo	*	*	*
Na-23	G	G	F	Ba-138	F	F	F
Mg	G	F	F	Ta-181	P+	P	P
Al-27	G	G	F	W-182	P	P	P
Si	G	G	G	W-184	P	P	P
P-31	G	G	F	W-185	P	P	P
S-32	G	G	F	W-186	P	P	P
Cl	*	G	*	Pb	*	G	F

*Tests masked by element effect

+Possibly masked by internal conversion

multistep Hauser-Feshbach/preequilibrium model codes that permit rather complete calculations in the 1-40 MeV region. Additionally, problems with energy balance in ENDF/B-V evaluations are noted, and we conclude that more consistent use of theory in evaluations is needed so that total energy conservation is maintained.

Time and space limitations have dictated that the scope of this paper be limited. There are many other developments that should lead to further improvement in theoretical calculations. More sophisticated fission models as described by Lynn,[36] Back et al.,[37] and Delagrange et al.[38] are planned or in use in certain model codes, and advances are being made in preequilibrium theory which offer promise of more accurate analyses in the future. Efforts to base model calculations on more fundamental theories, particularly regarding microscopic descriptions of nuclear level densities[39] and the optical model,[40] show promise for applied usage. An improved theoretical description of neutron energy spectra from fission has been developed,[41] and a new "master" code that will combine and refine some of the models presently used is under development at Lawrence Livermore Laboratory.[42]

Finally, progress in developing a unifed theory to include both Hauser-Feshbach and direct reaction mechanisms has been made in recent years,[43,44] and multistep direct reaction calculations as carried out by Tamura et al.[45] might prove useful in extending the evaluated date base to higher energies.

References

1. L. Stewart and P. G. Young, Trans. Am. Nucl. Soc. 23, 22 (1976).

2. D. C. Dodder and G. M. Hale, "Application of Approximate Isospin Conservation in R-Matrix Analysis," Proc. of Intnl. Conf. on Neutron Physics and Nuclear Data for Reactors and Other Applied Purposes," Harwell, England (Sept. 1978), p. 490.

3. G. M. Hale, Bull. Am. Phys. Soc. 24, 881 (1979).

4. D. Wilmore and P. E. Hodgson, Nucl. Phys. 55, 673 (1964).

5. F. G. Perey, Phys. Rev. 131, 745 (1962).

6. F. D. Becchetti, Jr., and G. W. Greenlees, Phys. Rev. 182, 1190 (1969).

7. D. G. Madland and P. G. Young, "Neutron-Nucleus Optical Potential for the Actinide Region," Proc. of Intnl. Conf. on Neutron Physics and Nuclear Data for Reactors and Other Applied Purposes," Harwell, England (Sept. 1978), p. 349.

8. J. P. Delaroche, Ch. Lagrange, and J. Salvy, "The Optical Model with Particular Considerations of the Coupled-Channel Optical Model," IAEA-190 (1976), p. 251.

9. Ch. Lagrange, Bull. Am. Phys. Soc. 24, 870 (1979).

10. G. Haouat et al., "Differential Cross Section Measurements of Fast Neutron Scattering for ^{208}Pb, ^{232}Th, and ^{238}U at 2.5 MeV," NEANDC(E)180 "L" (1977).

11. G. Haouat et al., "Differential Cross Section Measurements for 3.4-MeV Neutron Scattering from ^{208}Pb, ^{232}Th, ^{235}U, ^{238}U, and ^{239}Pu," NEANDC(E)196 "L" (1978).

12. D. G. Gardner

12. D. G. Gardner and M. A. Gardner, Bull. Am. Phys. Soc. 22, 993 (1977).

13. F. M. Mann, "HAUSER-4: A Computer Code to Calculate Nuclear Cross Sections," HEDL-TME-76-80 (1976).

14. C. Y. Fu, "Development of a Two-Step Hauser-Feshbach Code with Precompound Decays and Gamma-Ray Cascades: A Theoretical Tool for Cross Section Evaluation, Proc. Nucl. Cross Section Tech. Conf., Washington, D.C. (March 1975), NBS Special Publication 425, p. 328.

15. M. Uhl and B. Strohmaier, "STAPRE: A Computer Code for Particle-Induced Activation Cross Sections and Related Quantities," IRK 76/01 (1976).

16. P. G. Young and E. D. Arthur, "GNASH: A Preequilibrium Statistical Nuclear Model Code for Calculation of Cross Sections and Emission Spectra," LA-6947 (1977).

17. C. L. Dunford, "A Unified Model for Analysis of Compound Nucleus Reactions," AI-AEC-12931 (1970).

18. E. D. Arthur, "Calculation of Neutron Cross Sections on Isotopes of Yttrium and Zirconium," LA-7789-MS (1979).

19. C. Y. Fu, Bull. Am. Phys. Soc. 24, 884 (1979).

20. E. D. Arthur, "Comparison of Cross Sections Calculated with Various Statistical Model Codes Using Identical Parameter Sets," in "Applied Nuclear Data Research and Development, July 1-Sept. 30, 1978," compiled by C. I. Baxman and P. G. Young, LA-7596-PR (1978).

21. F. M. Mann and R. E. Schenter, "HEDL Evaluation of Actinide Cross Sections for ENDF/B-V," HEDL-TME-77-54 (1977).

22. C. Y. Fu, Atomic Data and Nucl. Data Tables 17, 127 (1976).

23. C. Y. Fu and F. G. Perey, ENDF/B-V evaluation MAT 1326, personal communication through the National Nuclear Data Center, Brookhaven National Laboratory (1979).

24. C. Y. Fu and F. G. Perey, Atomic Data and Nuclear Data Table 16, 409 (1975).

25. C. Y. Fu and F. G. Perey, J. Nucl. Materials 61, 153 (1976).

26. D. G. Gardner and M. A. Gardner, Bull. Am. Phys. Soc. 22, 615 (1977).

27. D. R. Nethaway and D. G. Gardner, Bull. Am. Phys. Soc. 22, 615 (1977).

28. M. Uhl and W. Matthes, Nucl. Sci. and Eng. 65, 368 (1978).

29. E. D. Arthur and P. G. Young, Bull. Am. Phys. Soc. 24, 863 (1979).

30. E. D. Arthur and C. A. Philis, Bull. Am. Phys. Soc. 24, 871 (1979).

31. L. R. Veeser and E. D. Arthur, "Measurements of (n,3n) Cross Sections for ^{235}U and ^{238}U," Proc. of Intnl. Conf. on Neutron Physics and Nuclear Data for Reactors and Other Applied Purposes, Harwell, England (Sept. 1978), p. 1054.

32. G. T. Chapman et al., "A Re-Measurement of the Neutron Induced Gamma-Ray Production Cross Sections for Iron in the Energy Range 850 keV $\leq E_n \leq$ 20.0 MeV," ORNL/TM-5416 (1976).

33. D. M. Drake et al., Nucl. Sci. and Eng. 65, 49 (1978).

34. C. Kalbach, personal communication (1979).

35. R. E. MacFarlane, "Energy Balance of ENDF/B-V," to be presented at the ANS Winter Meeting, San Francisco, (Nov. 1979).

36. J. E. Lynn, "Cross Section Theory for Actinide Nuclei," Proc. of Intnl. Conf. on Neutron Physics and Nuclear Data for Reactors and Other Applied Purposes, Harwell, England (Sept. 1978), p. 941.

37. B. B. Back et al., Phys. Rec. C10, 1948 (1974); see also Phys. Rec. C9, 1924 (1974).

38. H. Delagrange et al., Phys. Rec. C17, 1706 (1978).

39. L. G. Morretto, Nucl. Phys. A185, 145 (197).

40. J. P. Jeukenne et al., Phys. Rec. C16, 80 (1977).

41. D. G. Madland and J. R. Nix, Bull. Am. Phys. Soc. 24, 885 (1979); see also, Trans. Am. Nucl. Soc. 32, 726 (1979).

42. D. G. Gardner, personal communication (1979).

43. P. A. Moldauer, Phys. Rev. C12, 744 (1975).

44. H. M. Hofmann et al., Annals of Physics 90, 403 (1975).

45. T. Tamura et al., Phys. Lett. 66B, 109 (1977).